Dynamics of an Integral Membrane Peptide: A Deuterium NMR Relaxation Study of Gramicidin

R. Scott Prosser and James H. Davis
Department of Physics, University of Guelph, Guelph, Ontario N1G 2W1, Canada

ABSTRACT Solid state deuterium (^{2}H) NMR inversion-recovery and Jeener-Broekaert relaxation experiments were performed on oriented multilamellar dispersions consisting of 1,2-dilauroyl-*sn*-glycero-3-phosphatidylcholine and ^{2}H exchange-labeled gramicidin D, at a lipid to protein molar ratio (L/P) of 15:1, in order to study the dynamics of the channel conformation of the peptide in a liquid crystalline phase. Our dynamic model for the whole body motions of the peptide includes diffusion of the peptide around its helix axis and a wobbling diffusion around a second axis perpendicular to the local bilayer normal in a simple Maier-Saupe mean field potential. This anisotropic diffusion is characterized by the correlation times, $\tau_{R\|}$ and $\tau_{R\perp}$. Aligning the bilayer normal perpendicular to the magnetic field and graphing the relaxation rate, $1/T_{1Z}$, as a function of $(1 - S^2_{N-^2H})$, where $S^2_{N-^2H}$ represents the orientational order parameter, we were able to estimate the correlation time, $\tau_{R\|}$, for rotational diffusion. Although in the quadrupolar splitting, which varies as $(3\cos^2\theta_D - 1)$, has in general two possible solutions to θ_D in the range $0 \leq \theta_D \leq 90°$, the $1/T_{1Z}$ vs. $(1 - S^2_{N-^2H})$ curve can be used to determine a single value of θ_D in this range. Thus, the $1/T_{1Z}$ vs. $(1 - S^2_{N-^2H})$ profile can be used both to define the axial diffusion rate and to remove potential structural ambiguities in the splittings. The T_{1Z} anisotropy permits us to solve for the two correlation times ($\tau_{R\|} = 6.8 \times 10^{-9}$ s and $\tau_{R\perp} = 6 \times 10^{-6}$ s). The simulated parameters were corroborated by a Jeener-Broekaert experiment where the bilayer normal was parallel to the principal magnetic field. At this orientation the ratio, $J_2(2\omega_0)/J_1(\omega_0)$ was obtained in order to estimate the strength of the restoring potential in a model-independent fashion. This measurement yields the rms angle, $\langle\theta^2\rangle^{1/2}$ ($= 16 \pm 2°$ at 34°C), formed by the peptide helix axis and the average bilayer normal.

INTRODUCTION

Protein dynamics spans a wide range of amplitudes (0.01–100 Å), energies (0.1–100 kcal/mol), and time scales (10^{-15} to 10^3 s) (Brooks et al., 1988). This motional freedom implies that a native protein adopts a wide distribution of conformations, which is believed to be intrinsically related to its function (Brooks et al., 1988; McCammon and Harvey, 1987). Membrane proteins also undergo whole-body motions which may also significantly influence their function (Knowles and Marsh, 1991). Solid state NMR is ideally suited to the study of dynamics in such partially ordered systems. In particular, two deuteron spin-lattice relaxation times (T_{1Z} and T_{1Q}) can be measured which in turn yield the spectral density function, $J(\omega)$, in the Redfield limit. The spectral density, which is the Fourier transform of the correlation function, provides a statistical mechanical representation of the molecular dynamics. Fortunately, not all of the motions of the transmembrane peptide will be relaxation effective. T_{1Z} and T_{1Q} are most sensitive to motions whose characteristic correlation times are on the order of the inverse of the Larmor frequency, ω_0 ($= 2\pi \times 55.265$ MHz), while the spectral lineshapes reveal information about motions on the time scale of the inverse of the quadrupole coupling constant, $e^2qQ/\hbar$($\approx$200 kHz). The dynamic processes which we will consider will have characteristic correlation times, τ_c, in the range $10^{-10}\,\text{s} < \tau_c < 10^{-4}\,\text{s}$. It is likely that such time scales encompass processes such as whole body rotational diffusion, wobbling of the peptide about the local bilayer normal in a restoring potential, collective order director fluctuations, and possible internal motions such as side chain reorientations and internal helical librations (Venkatachalam and Urry, 1984). The formalism used in the analysis of spin-lattice relaxation experiments depends upon the time scale(s) of the motion(s) (relative to $(e^2qQ/\hbar)$ and ω_0) and the nature of the coupling of the spin system to the lattice. For our purposes, a semiclassical approach will be sufficient to describe the evolution of the spin system and its interaction with the lattice. We will briefly review this formalism, then systematically develop expressions for spin-lattice relaxation rates (T_{1Z} and T_{1Q}) assuming two models for the dynamics of an amphiphilic peptide, gramicidin A, in oriented phospholipid multilamellar dispersions:

1. Simple rotational diffusion of the rigid peptide around its helix axis, and
2. Restricted diffusion (characterized by the correlation times, $\tau_{R\|}$ and $\tau_{R\perp}$) in a restoring potential whose strength determines the molecular order parameter, S_{mol} (Mayer et al., 1988, 1990; Prosser et al., 1992).

We will then discuss the correspondence between the models and our relaxation data, and strategies for distinguishing between motional models. Few detailed experimental measurements of transmembrane peptide dynamics exist to date. Maximum values of rotational correlation times, $\tau_{R\|}$ ($= 1/6D_\|$), have been measured by ESR on spin-labeled proteins. These values range from 25 to 2 μs for the integral membrane proteins, Na, K-ATPase and the ADP-ATP

Received for publication 15 June 1993 and in final form 16 February 1994.
Address reprint requests to J. H. Davis, Department of Physics, University of Guelph, Guelph, Ontario, Canada N1G 2W1.
Present address (R. S. P.): Institut für Physikalische Chemie, der Universität Stuttgart, Pfaffenwaldring 55, D-70569 Stuttgart, Germany.

0006-3495/94/05/1429/12 $2.00

carrier, whose molecular masses are 147 and 39 kDa, respectively (Knowles and Marsh, 1991). Knowles and Marsh (1991) suggest that membrane proteins undergo little or no wobble. NMR order parameter analysis of the integral membrane peptide, gramicidin A, by Separovic et al. (1993), suggests that the rms angle formed by the peptide helix axis with the average bilayer normal, is about 12.5°, implying a significant amplitude of wobble. Our measurements using ^{2}H NMR spectroscopy of exchange-labeled gramicidin D also suggests a wobble amplitude at least equal to this value.

Often spectroscopy is associated with structural information, while relaxation experiments are connected with dynamics. We will present a simple strategy for analyzing T_{1Z} or T_{1Q} relaxation data as a function of splitting (for a rigid molecule undergoing diffusion around its long axis in the membrane) that yields unambiguous structural information which cannot be obtained from spectra alone. This strategy is applicable even to systems in which diffusion about an axis perpendicular to the local bilayer normal (wobble) is significant.

THEORY

To begin the description of nuclear spin-lattice relaxation, we examine the evolution of the reduced density operator, $\sigma(t)$, which evolves under a spin Hamiltonian, $\mathscr{H}^s$, according to the Stochastic Liouville equation

$$\frac{d}{dt}\sigma(t) = \frac{i}{\hbar}[\mathscr{H}^s, \sigma(t)] - \Gamma(\sigma(t) - \sigma_0), \tag{1}$$

where Γ is the relaxation operator describing the interaction between the lattice and the spin system as $\sigma(t)$ returns to its equilibrium value, σ_0 $(= e^{-\mathscr{H}_z/kT}/\mathrm{tr}\{e^{-\mathscr{H}_z/kT}\}$, where $\mathscr{H}_Z$ is the Zeeman Hamiltonian). Here, $\sigma(t)$ and $\mathscr{H}^s$ are obtained, from the complete density operator and full Hamiltonian, by taking the trace over the lattice coordinates. In the absence of ratio frequency (rf) fields or dipolar interactions, and neglecting the chemical shift interaction,

$$\mathscr{H}^s = \mathscr{H}_Z + \langle\mathscr{H}_Q(t)\rangle_t + (\mathscr{H}_Q(t) - \langle\mathscr{H}_Q(t)\rangle_t), \tag{2}$$

where $\mathscr{H}_Q(t)$ is the quadrupolar Hamiltonian and $\langle\mathscr{H}_Q(t)\rangle_t$ represents its time-average. We will refer to the fluctuating part of this Hamiltonian as $\mathscr{H}_r$ $(= \mathscr{H}_Q(t) - \langle\mathscr{H}_Q(t)\rangle_t)$. The quadrupolar Hamiltonian, $\mathscr{H}_Q(t)$, may be written in terms of the scalar product of two second-rank spherical tensors (Davis, 1983)

$$\mathscr{H}_Q(t) = C_Q \sum_{m=-2}^{+2} (-1)^m T_{2,m} F_{2,-m}(t), \tag{3}$$

where $C_Q = eQ/2$, so that

$$\begin{aligned}\mathscr{H}_r(t) &= (\mathscr{H}_Q(t) - \langle\mathscr{H}_Q(t)\rangle_t) \\ &= C_Q \sum_{m=-2}^{+2} (-1)^m T_{2,m}(F^L_{2,-m}(t) - \langle F^L_{2,-m}(t)\rangle_t).\end{aligned} \tag{4}$$

$T_{2,m}$ contains only spin operators and $F^L_{2,m}$ represents the electric field gradient (EFG) tensor transformed into the laboratory frame. The spin operators, $T_{2,m}$, in the laboratory frame where the axis of quantization (z axis) is defined in the direction of B_0, and the EFG tensor in its principal axis system (PAS), may be written explicitly as (Davis, 1983)

$$\begin{aligned} T_{2,0} &= \frac{1}{\sqrt{6}}[3I_z^2 - I(I+1)] & F^{PAS}_{2,0} &= \sqrt{3/2}\,\mathrm{eq} \\ T_{2,+1} &= \mp 1/2[I_zI_\pm + I_\pm I_z], & F^{PAS}_{2,\pm1} &= 0 \\ T_{2,+2} &= 1/2 I_\pm^2 & F^{PAS}_{2,\pm2} &= 1/2\,\mathrm{eq}\eta. \end{aligned} \tag{5}$$

The EFG tensor may be transformed into the lab frame using the Wigner rotation matrix $\mathscr{D}^{(2)}_{m'm}(\alpha, \beta, \gamma)$ to give

$$F^L_{2,m} = \sum_{m'=-2}^{2} F^{PAS}_{2,m'}\mathscr{D}^{(2)}_{m'm}(\alpha\beta\gamma). \tag{6}$$

Transforming to an interaction representation and using second order perturbation theory, we may write (Davis, 1983; Jeffrey, 1981)

$$\begin{aligned}&\frac{d}{dt}\sigma^*(t) \\ &= -\frac{i}{\hbar}[\langle\mathscr{H}_Q\rangle_t, \sigma^*] - \frac{C_Q}{\hbar^2}\sum_{m=-2}^{2}[T_{2,m}, [T_{2,-m}, \sigma^*(t) - \sigma_0^*]] \\ &\times \int_0^\infty d\tau e^{im\omega_0\tau}\overline{(F^L_{2,-m}(t)F^L_{2,m}(t-\tau) - \langle F^L_{2,-m}(t)\rangle_t^2)},\end{aligned} \tag{7}$$

where only the secular terms have been retained. In this semiclassical approach, the evolution of the spin system is described quantum mechanically by the density operator, while the lattice dynamics are visualized classically as a fluctuating random process. We next define a correlation function, $G_m(\tau)$, for this random process as

$$G_m(\tau) = \overline{(F^L_{2,-m}(t)F^L_{2,m}(t-\tau) - \langle F^L_{2,-m}(t)\rangle_t^2)} \tag{8}$$

characterized by a correlation time, τ_c, and a spectral density function,

$$J_m(m\omega) = (-1)^m \int_{-\infty}^{\infty} d\tau e^{im\omega\tau} G_m(\tau). \tag{9}$$

Comparing our result with Eq. 1 we see that the relaxation operator, Γ, may be written as

$$\begin{aligned}&\Gamma(\sigma^*(t) - \sigma_0^*) \\ &= \frac{C_Q^2}{2\hbar^2}\sum_{m=-2}^{2}(-1)^m[T_{2,m}, [T_{2,-m}, \sigma^*(t) - \sigma_0^*]]J_m(m\omega).\end{aligned} \tag{10}$$

For a spin-one system, the density operator may be expressed in terms of a unity operator and eight other orthonormal operators, $\{\mathscr{Q}_p\}$, such that $\sigma^*(t) = \sum_p c_p(t)\mathscr{Q}_p$, where only the coefficients, $c_p(t)$, are time-dependent. Making use of the property that $\mathrm{tr}\{\mathscr{Q}_p\mathscr{Q}_q\} = \delta_{pq}$, Eq. 7 can be written in

terms of a system of coupled linear first order differential equations which relate the decay rate of various components of the density matrix to the spectral density function. For example, it can be shown that the Zeeman order and quadrupolar order decay exponentially with respective rates $1/T_{1Z}$ and $1/T_{1Q}$ given by (Davis, 1983; Jeffrey, 1981)

$$\frac{1}{T_{1Z}} = \frac{1}{8}\left(\frac{eQ}{\hbar}\right)^2 (J_1(\omega_0) + 4J_2(2\omega_0))$$
$$\frac{1}{T_{1Q}} = \frac{1}{8}\left(\frac{eQ}{\hbar}\right)^2 3J_1(\omega_0) \qquad (11)$$

Thus, by performing inversion-recovery and Jeener-Broekaert experiments, we can measure both T_{1Z} and T_{1Q} and directly relate these quantities to the spectral density functions, which in turn describe the motion(s) of interest. We emphasize that the above treatment is valid only as long as $\tau_c \ll t, T_1, T_2$. The strategy, within this limit, is to postulate a particular motional model and calculate its correlation function, which can then be related to T_{1Z} and T_{1Q}. By making use of the Wigner rotation matrices and successive transformations, the correlation function becomes straightforward to calculate. The transformations used to describe anisotropic diffusion of a peptide in a membrane are defined in Fig. 1 and may be summarized as follows:

1. The EFG tensor is first transformed (by the Euler angles $\{\phi_D, \theta_D, \psi_D\}$) from its PAS to the molecular diffusion tensor system, in which the Z axis is along the peptide helix axis.

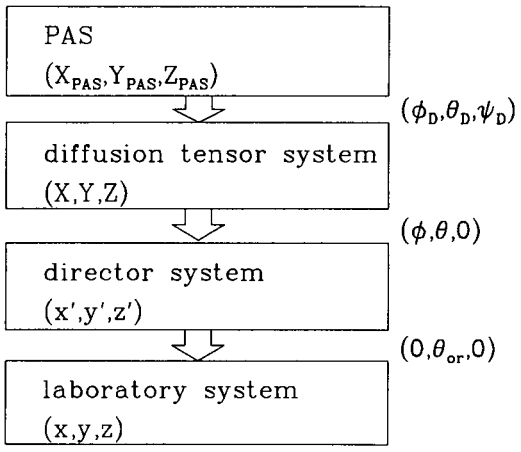

FIGURE 1 Notation for coordinate systems and Euler transformations used in the NMR relaxation model. The coordinate systems are as follows: PAS $\{X_{PAS}, Y_{PAS}, Z_{PAS}\}$ (the Z_{PAS} axis is generally along the C—^{2}H or N—^{2}H bond when the asymmetry parameter, η, is zero), diffusion tensor system $\{X, Y, Z\}$ (Z = helix axis; origin in channel center with the X axis passing through the C_α atom of Val_1 such that Y and Z equal zero at this point), director system $\{x', y', z'\}$ (z' = locally averaged bilayer normal), and the laboratory system $\{x, y, z\}$ (the z axis along the principal magnetic field, B_0). Note that for axial diffusion only ϕ is time dependent while $\theta = 0$; for diffusion about an axis perpendicular to the locally averaged bilayer normal $\theta = \theta(t)$. The Euler angles $\{\alpha, \beta, \gamma\}$ define rotations by α about the original z axis, then by β about the resultant y axis, and finally by γ about the resultant z axis.

2. The Euler angles $\{\phi, \theta, 0\}$ accomplish the next transformation to the director system, in which the z' axis is along the local bilayer normal, and
3. The Euler angles $\{0, \theta_{or}, 0\}$ specify the final transformation to the laboratory frame (z axis along the principal magnetic field). θ_{or} specifies the angle between the normal to the glass plates and the magnetic field.

The notation of Fig. 1 will next be used to derive expressions for diffusion around a single axis (parameterized by a single correlation time) and anisotropic diffusion in an orienting potential (parameterized by two correlation times).

Diffusion around a single axis:

For simple diffusion of the peptide around its helix axis, only the azimuthal angle, ϕ, is time dependent, while $\theta = 0$. In this case, the correlation function may be written as

$$\overline{(F^L_{2,-m}(t)F^L_{2,m}(t-\tau)} \qquad (12)$$
$$= \sum_{m_1,m_2,m_3,m_4} F^{PAS}_{2,m_1}F^{PAS}_{2,m_2}\mathscr{D}^{(2)}_{m_1,m_3}(\phi_D, \theta_D, \psi_D)\mathscr{D}^{(2)}_{m_2,m_4}(\phi_D, \theta_D, \psi_D)$$
$$\times d^{(2)}_{m_4,-m}(\theta_{or})d^{(2)}_{m_3,m}(\theta_{or})\overline{e^{-im_4\phi(t)}e^{-im_3\phi(t-\tau)}},$$

where $\mathscr{D}^{(2)}_{m_4,-m}(\phi(t), \theta_{or}, 0) = e^{-im_4\phi(t)}d^{(2)}_{m_4,-m}(\theta_{or})$ (Davis, 1983, 1993). Making use of the fact that the above correlation function is non-zero if $m_4 = -m_3$ and assuming that $g_{m_3}(\tau) = \overline{e^{im_3\phi(t)}e^{-im_3\phi(t-\tau)}} = \exp(-|\tau|/\tau_{m_3})$, we may write

$$J_m(m\omega)$$
$$= (-1)^m \sum_{m_1,m_2,m_3} F^{PAS}_{2,m_1}F^{PAS}_{2,m_2}\mathscr{D}^{(2)}_{m_1,m_3}(\phi_D, \theta_D, \psi_D) \qquad (13)$$
$$\times \mathscr{D}^{(2)}_{m_2,-m_3}(\phi_D, \theta_D, \psi_D)d^{(2)}_{-m_3,-m}(\theta_{or})d^{(2)}_{m_3,m}(\theta_{or})j(\tau_{m_3}, m\omega),$$

where

$$j(\tau_{m_3}, m\omega) = \frac{2\tau_{m_3}}{1 + m^2\omega^2\tau^2_{m_3}}, \qquad \tau_{m_3} = \frac{1}{m^2_3 D} \qquad (14)$$

and where D represents a diffusion rate. The temperature dependence of $J_m(m\omega)$ (and hence the relaxation times) arises from the Arrhenius temperature dependence of the correlation times, τ_{m_3}, where

$$\tau_1 = \tau^0_1 e^{E_A/RT} \qquad \tau_1 = 1/D. \qquad (15)$$

E_A is the activation energy, in units of J/mol, for axial diffusion, and R is the gas constant. Thus a completely analytical expression can be written for the spectral density function, $J_m(m\omega)$. The strategy, then, in simulating the relaxation data, is to first simulate the spectrum to determine the time-independent parameters (i.e., ϕ_D, θ_D, ψ_D, η, and $e^2qQ/\hbar$) for each ^{2}H exchange label (Prosser et al., 1994), then adjust τ^0_1 and E_A, which must predict T_{1Z} and T_{1Q} for all values of temperature, θ_D, and θ_{or}.

For deuterons, the principal component of the EFG tensor generally lies along, or very nearly along, the C—D, O—D, or N—^{2}H bonds (Vold and Vold, 1991). For ^{2}H in C—^{2}H bonds, the EFG is nearly axially symmetric ($\eta \approx 0.01$–0.02)

(Millar et al., 1986). However, within peptides for ^2H in N—^2H bonds, η may be as high as 0.2 (Prosser et al., 1994; Vold and Vold, 1991), leading to experimentally significant relaxation effects. In the simpler case where $\eta = 0$, the expression for the spectral densities becomes (Davis, 1983, 1993)

$$J_m(m\omega) = (-1)^m \frac{4\pi}{5}(F_{2,0}^{PAS})^2 \sum_{m'=-2}^{2} d^{(2)}_{m',m}(\theta_{or}) d^{(2)}_{-m',-m}(\theta_{or}) \times Y^*_{2,-m'}(\theta_D, 0) Y^*_{2,m'}(\theta_D, 0) j(\tau_{m'}, m\omega), \quad (16)$$

where $Y_{2,m'}(\theta, \phi)$ represent the spherical harmonic functions (Jackson, 1975). This can be further simplified in the case of oriented samples where $\theta_{or} = 90°$. Under such circumstances we obtain the following

$$J_1(\omega) = \tfrac{3}{4}(F_{2,0}^{PAS})^2[\sin^2\theta_D \cos^2\theta_D j(\tau_1, \omega_0) + \tfrac{1}{4}\sin^4\theta_D j(\tau_2, \omega_0)]$$

$$J_2(2\omega) = \tfrac{3}{4}(F_{2,0}^{PAS})^2[\sin^2\theta_D \cos^2\theta_D j(\tau_1, 2\omega_0) + \tfrac{1}{16}\sin^4\theta_D j(\tau_2, 2\omega_0)], \quad (17)$$

such that (Davis, 1993)

$$\frac{1}{T_{1Z}} = \frac{1}{8}\left(\frac{3e^2qQ}{4\hbar}\right)^2 [2\sin^2\theta_D \cos^2\theta_D j(\tau_1, \omega_0) + \tfrac{1}{2}\sin^4\theta_D j(\tau_2, \omega_0) + 8\sin^2\theta_D \cos^2\theta_D j(\tau_1, 2\omega_0) + \tfrac{1}{2}\sin^4\theta_D j(\tau_2, 2\omega_0)]. \quad (18)$$

Anisotropic diffusion in an orienting potential

It seems likely that an integral membrane peptide will be acted upon by a restoring potential similar to those which act upon lipid or liquid crystal molecules (Vold and Vold, 1988). Accordingly, we will use a simple Maier-Saupe orienting potential, as is common in molecular theories of liquid crystals (Cotter, 1977). In the case of an axially symmetric order tensor, which is a good approximation for gramicidin in a fluid bilayer phase (Separovic et al., 1993), only one adjustable parameter, A_{00}, enters the orientational distribution function (Mayer, et al., 1990)

$$f(\theta) = N \exp[A_{00}\mathscr{D}^2_{00}(0, \theta, 0)], \quad (19)$$

where $\mathscr{D}^2_{00}(0, \theta, 0)$ is an element of the second rank Wigner rotation matrix and N represents a normalization constant. A_{00} thus characterizes the orientation of the peptide with respect to the local director. The orientational order parameter, S_{ZZ}, is in turn related to the coefficient, A_{00}, by a mean value integral (Mayer et al., 1990):

$$S_{ZZ} = N \int_0^\pi \mathscr{D}^2_{00}(0, \theta, 0)\exp[A_{00}\mathscr{D}^2_{00}(0, \theta, 0)]\sin\theta\, d\theta. \quad (20)$$

Thus, the molecular order of the peptide is specified by the orientational order parameter, S_{ZZ}, and the peptide may be visualized as undergoing continuous anisotropic diffusion in an orienting potential. The dynamics of this diffusional process are illustrated in Fig. 2 and are characterized by the correlation times, $\tau_{R\|}$ and $\tau_{R\perp}$, which correspond to diffusion around the helix axis and diffusion around an axis perpendicular to the local bilayer normal.

In deriving the correlation function for anisotropic diffusion, we assume that the diffusional process can be described by a master equation (Mayer et al., 1990; Wittebort and Szabo, 1978)

$$\frac{\partial p_i(t)}{\partial t} = \sum_{j=1}^{N} p_j(t) W_{j,i}, \quad (21)$$

where $p_j(t)$ represents the probability that the peptide occupies configuration Ω_j at time t and the Markov operator, $W_{j,i}$, represents the transition rate from site Ω_j to Ω_i. The particular values for W_{ij} are obtained from the following expressions which apply to anisotropic diffusion in an orienting potential, under the assumption of microscopic reversibility and under equilibrium conditions ($W_{i,i} = -\sum_{j\neq i} W_{i,j}$) (Mayer et al., 1988, 1990):

$$W_{i,i+1} + W_{i,i-1} = (3\Delta^2\tau_R)^{-1}$$
$$W_{i,j}p_i^{eq} = W_{j,i}p_j^{eq} \quad (22)$$
$$W_{i,i} = -(3\Delta^2\tau_R)^{-1}$$

where Δ represents the angular separation of adjacent sites, and τ_R represents either $\tau_{R\|}$ or $\tau_{R\perp}$.[1] The equilibrium probability, p_i^{eq}, is in turn determined by integrating the relative area of site i in the above orientational distribution function, $f(\theta)$.

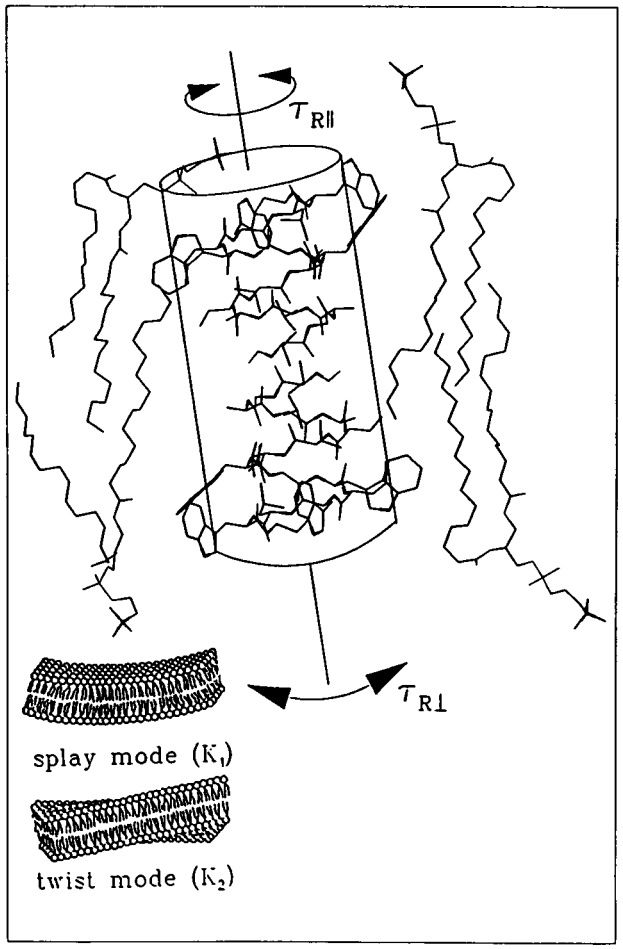

FIGURE 2 Gramicidin A in a fluid phase phospholipid bilayer. $\tau_{R\|}$ and $\tau_{R\perp}$ represent correlation times for whole body diffusion around the helix axis and an axis perpendicular to the local bilayer normal, respectively. The inset to this figure illustrates collective order-director fluctuations, which are expected to occur in the low frequency realm. (Inset taken from Rommel et al. (1988), with permission).

[1] The correlation time, $\tau_{R\|}$, which corresponds to diffusion around the helix axis, may be compared with the axial diffusion rate, D, using the relation $D = 1/(6\tau_{R\|})$.

Our goal is to solve the master equation and derive an expression for the autocorrelation function, $G_m(t)$, given by

$$G_m(t) = (C_Q F^{PAS}_{2,0})^{-2} \overline{F^{L*}_{2,m}(0) F^{L}_{2,m}(t)}. \quad (23)$$

The EFG tensor, in the laboratory frame, $F^L_{2,m}$, may in turn be written in terms of a product of its PAS components and three Wigner rotation matrices

$$F^L_{2m} = \sum_{m_1,m_2,m_3=-2}^{2} F^{PAS}_{2,m_3} \mathscr{D}^{(2)}_{m_3,m_2}(\phi_D, \theta_D, \psi_D) \mathscr{D}^{(2)}_{m_2,m_1}(\phi, \theta, 0) \mathscr{D}^{(2)}_{m_1,m}(0, \theta_{or}, 0), \quad (24)$$

where only θ and ϕ are time-dependent. Wittebort and Szabo (1978) have shown that the substitution $p_i = X_i e^{-\lambda t}$ converts the master equation into an eigenvalue equation. Furthermore, by making the transformations (Wittebort and Szabo, 1978)

$$\tilde{W}_{i,j} = (W_{i,j} W_{j,i})^{1/2} \qquad \tilde{X}_i = (p^{eq}_i)^{-1/2} X_i, \quad (25)$$

we obtain

$$\tilde{\mathbf{W}}\tilde{\mathbf{X}} = -\lambda \tilde{\mathbf{X}}. \quad (26)$$

In this case, the eigenvalues, λ^k, are real and $\tilde{\mathbf{W}}$ has a zero eigenvalue whose corresponding eigenvector, $\tilde{\mathbf{X}}^0$, is related to the equilibrium distribution by (Wittebort and Szabo, 1978)

$$\tilde{X}^0_i = (p^{eq}_i)^{1/2}. \quad (27)$$

Wittebort and Szabo also point out that the conditional probability, $p(i, t \mid j, 0)$, (i.e., the probability that the peptide occupies site i at a time t, given that it occupied site j at $t = 0$) may be expressed as

$$p(i, t \mid j, 0) = \tilde{X}^0_i (\tilde{X}^0_j)^{-1} \sum_k \tilde{X}^k_i \tilde{X}^k_j \exp(-\lambda^k t). \quad (28)$$

Using the expressions for p^{eq}_i and $p(i, j \mid j, 0)$ from Eqs. 27 and 28, we arrive an expression for the autocorrelation function (Mayer et al., 1990)

$$G_m(t) = (C_Q F^{PAS}_{2,0})^{-2} \sum_{i,j} F_{2,m}(\Omega_i) F^*_{2,m}(\Omega_j) \tilde{X}^0_i \tilde{X}^0_j \sum_k \tilde{X}^k_i \tilde{X}^k_j \exp(-\lambda^k t), \quad (29)$$

whose Fourier transform gives the desired spectral density function

$$J_m(\omega) = (C_Q F^{PAS}_{2,0})^{-2} \sum_{i,j} F_{2,m}(\Omega_i) F^*_{2,m}(\Omega_j) \tilde{X}^0_i \tilde{X}^0_j \sum_k \tilde{X}^k_i \tilde{X}^k_j \frac{2\lambda^k}{(\lambda^k)^2 + \omega^2}. \quad (30)$$

T_{1Z} and T_{1Q} are then obtained from Eq. 11.

MATERIALS AND METHODS

Our sample preparation procedure was exactly the same as described in a previous paper (Prosser et al., 1994). We will only repeat that the NMR pulse experiments included quadrupole echo (Davis et al., 1976), inversion-recovery, and modified Jeener-Broekaert pulse sequences, the details of which have been documented elsewhere (Davis, 1983; Vold and Vold, 1991). Each of these pulse sequences was preceded by a "soft" π pulse designed to selectively eliminate the water signal (or any spectral component very near to the center frequency). The quadrupole echo (QE), inversion-recovery (IR), and Jeener-Broekaert (JB) pulse sequences may be described as follows: QE: $[(\pi/2)_x - \tau_1 - (\pi/2)_y]$; IR: $[(\pi)_x - \tau_2 - (\pi/2)_x - \tau_1 - (\pi/2)_y]$; JB: $[(\pi/2)_x - \tau_3 - (\pi/4)_y - \tau_4 - (\pi/4)_y - \tau_1 - (\pi/2)_y]$. The particular phase cycling schemes for the above sequences may be found elsewhere (Vold and Vold, 1991). The JB sequence was modified in order to produce pure quadrupolar order, rather than quadrupolar order and double-quantum coherence (Davis, 1991). Typically, between 40,000 and 120,000 scans were accumulated (with the exception of the JB experiment in which 200,000 scans were obtained per spectrum) with a refocusing time, τ_1, equal to 35 μs, and a repetition time of 0.35 s. In the JB experiment, the parameter, τ_3, used to create quadrupolar order, was set such that $\omega_Q \tau_3 = \pi/2$, thus exciting quadrupolar order for a given splitting, $\Delta\nu_Q = \omega_Q/2\pi$. All spectra were taken in a magnetic field of 8.5T where $\nu_0 = 55.265$ MHz for ^{2}H.

Analysis and simulation of relaxation times

To determine T_{1Z}, free induction decays (FIDs) were recorded as a function of τ_2. The corresponding spectra were obtained for each value of τ_2. The decay of the area under a particular spectral component as a function of τ_2, was fitted to an exponential function, in which case the corresponding decay constant determined T_{1Z}. Similarly, T_{1Q} was determined by fitting the decay of the echo amplitude (as a function of τ_4) to an exponential.

Our studies on oriented exchange-labeled gramicidin D were confined to T_{1Z} and T_{1Q} in the liquid crystalline phase. Simulation of these relaxation times was accomplished either by evaluation of an analytical expression for rotational diffusion (Davis, 1993) about the helix axis, or by a numerical approximation to anisotropic diffusion in a Maier-Saupe reorienting potential (Mayer et al., 1988). The program used to estimate relaxation times for anisotropic diffusion employs 10 librational and 20 rotational sites (i.e., $\tilde{\mathbf{W}}$ is a 200 $\times$ 200 matrix) and calculates $J_1(\omega)$ and $J_2(2\omega)$ in less than a minute on an IBM RISC 6000 (the diagonalization requires a fraction of a second with most of the processing time consumed by the multiple summations).

RESULTS AND DISCUSSION

We begin our analysis by assuming that the main contribution to the observed spin-lattice relaxation rates is that of diffusion of the peptide around its helix axis (Davis, 1988). Furthermore, from Eq. 30, it can be shown that if whole-body diffusion perpendicular to the bilayer normal (wobble) was relaxation-effective (for typical values of θ_D which we expect in gramicidin), then its relative contribution to the spin-lattice relaxation rates would be minimized for plate orientations of $\theta_{or} = 90°$. Thus, a relaxation study at this angle permits us to focus on diffusion around the helix axis. Gramicidin possesses twenty ^{2}H exchangeable sites (and almost as many resolvable doublets in oriented lipid multilayers). It is useful to measure T_{1Z} (at $\theta_{or} = 90°$) as a function of the orientational order parameter, $S_{N—^2H}$, corresponding to each observable doublet, where we define $S_{N—^2H} = \frac{1}{2}(3\cos^2\theta_D - 1)$. We will ignore, for the moment, the effect of the nonzero asymmetry parameter, η. We emphasize that the orientational order parameter may be determined directly from the observed splitting, $\Delta\nu_Q$, such that $S_{N—^2H} = \Delta\nu_Q/[3e^2qQ/4h]$ (Prosser et al., 1994),[2] while for each resolvable doublet we can also measure T_{1Z} (or T_{1Q}). Thus, within the axial diffusion model, the curve defined by $1/T_{1Z}$ (or $1/T_{1Q}$) vs. $(1 - S^2_{N—^2H})$ completely determines the diffusion rate.

Fig. 3 displays theoretical profiles for $1/T_{1Z}$ and $1/T_{1Q}$ vs. $(1 - S^2_{N—^2H})$ for several values of the diffusion rate, D. A useful feature of these relaxation profiles is that for two values of θ_D, which would yield identical splittings, $\Delta\nu_Q$, the relaxation rates may be dramatically different. This is exemplified in Fig. 3 *a* where the relaxation rates for both $\theta_D = 90°$ and $\theta_D = 35.26°$ (whose corresponding splittings are identical) are clearly distinct. Although in general, the quadrupolar splitting, which is a function of $(3\cos^2\theta_D - 1)$, has two possible solutions to θ_D in the range $0 \leq \theta_D \leq 90°$, the $1/T_{1Z}$ vs. $(1 - S^2_{N—^2H})$ curve can be used to determine a single

[2] Additional motions which contribute to narrowing are presumed to scale all splittings by a common amount, while not contributing significantly to $1/T_1$ relaxation.

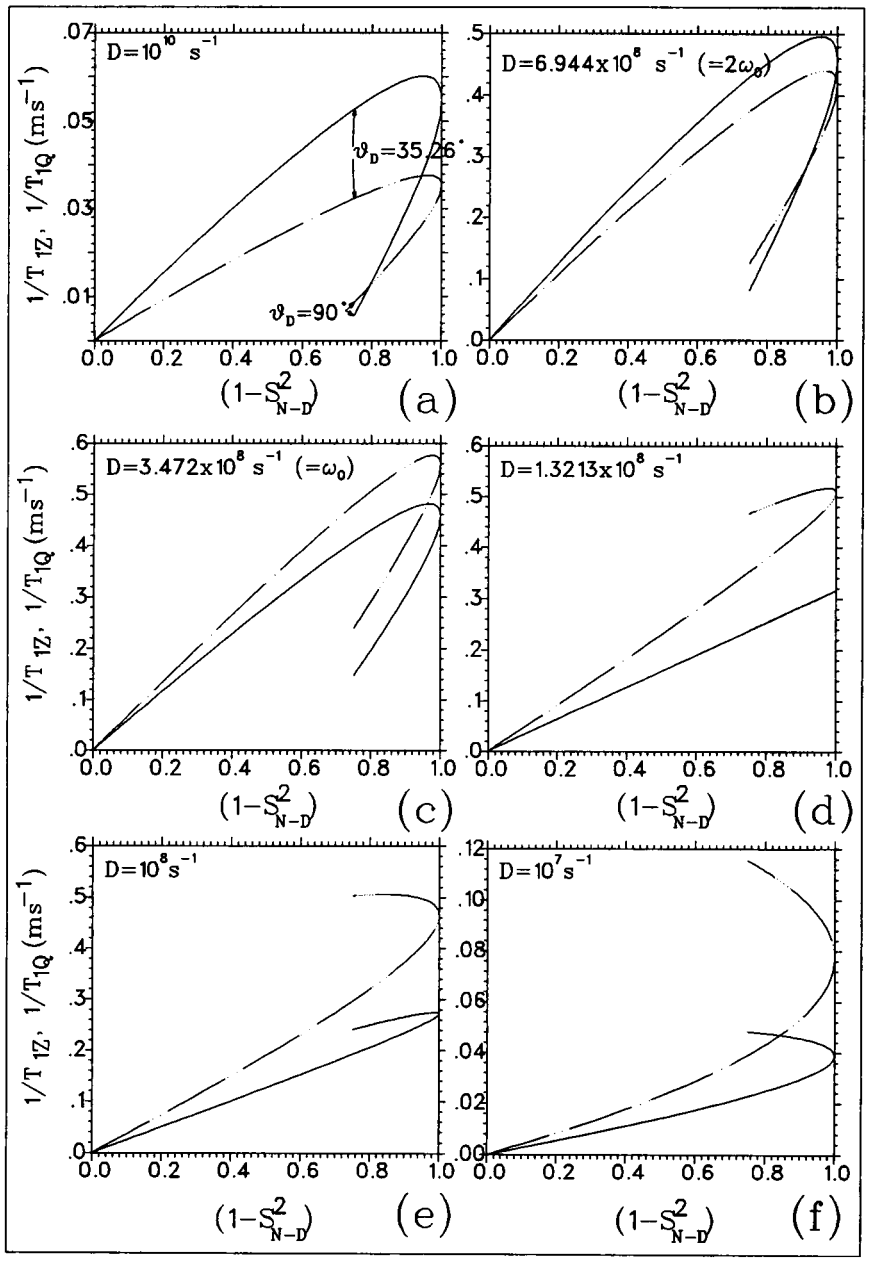

FIGURE 3 Theoretical relaxation rates, $1/T_{1Z}$ and $1/T_{1Q}$ as a function of $1 - S^2_{N-^2H}$ for long axis diffusion rates, D, equal to 10^{10} s^{-1} (*a*), 6.944×10^8 s^{-1} ($=2\omega_0$) (*b*), 3.472×10^8 s^{-1} ($=\omega_0$) (*c*), 1.3213×10^8 s^{-1} (*d*), 1.0×10^8 s^{-1} (*e*), and 1.0×10^7 s^{-1} (*f*). The solid and dashed lines represent the profiles for $1/T_{1Z}$ and $1/T_{1Q}$, respectively. The constants in this simulation are η (= 0), e^2qQ/h (=205.9 kHz), and ω_0 (=55.265 $\times 2\pi \times 10^6$ s^{-1}).

value of θ_D in this range. Thus, the $1/T_{1Z}$ vs. $(1 - S^2_{N-^2H})$ curve can be used both to define the diffusion rate and to remove potential structural ambiguities based on the splittings. T_{1Z} (or T_{1Q}) can be a useful quantity for determining structural constraints. Note in Fig. 3, *a–f*, that as the diffusion rate slows, the characteristic downward "hook" of $1/T_{1Z}$ and $1/T_{1Q}$ becomes linear (Fig. 3 *d*) and eventually becomes inverted (Fig. 3, *e* and *f*)). As long as a sample contains enough distinct labeled sites to define a characteristic $1/T_{1Z}$ (or $1/T_{1Q}$) vs. $(1 - S^2_{N-^2H})$ (or $1 - S^2_{C-^2H}$, etc.) curve, it is possible to determine the correlation time from a single spectrum. If these characteristic curves could be obtained as a function of temperature (over a broad enough range), one would expect to observe a sequence of profiles such as those predicted in Fig. 3.

Fig. 4 *a* features a spectrum of ^{2}H exchange-labeled GD from an inversion-recovery (T_{1Z}) experiment. In this spectrum, which was obtained at 65°C, one can clearly identify 11 doublets, each of which are labeled in the figure. In Fig. 4 *b* the relaxation rates ($1/T_{1Z}$), corresponding to each doublet, are graphed as a function of $(1 - S^2_{N-^2H})$. From this relaxation profile and Eq. 18, we obtain a diffusion rate of $1.58 \pm 0.15 \times 10^7$ s^{-1}, and from the y intercept we obtain an estimate for the contribution to relaxation due to either additional interactions (e.g., heteronuclear dipolar interactions) or motions (e.g., wobble of the diffusion axis). The four innermost doublets (8–11 in Fig. 4 *a*) all have splittings in which there are two possible solutions to θ_D in the region $\{0° \leq \theta_D \leq 90°\}$. Furthermore, by comparing our spectrum to that of Davis (1988), who identified the tryptophan indole peaks based on an analysis of the chemical shifts, we can tentatively assign peaks 7, 8, 9, and 11 as indole candidates. The profile in Fig. 4 *b* indicates that peaks 8, 10, and 11

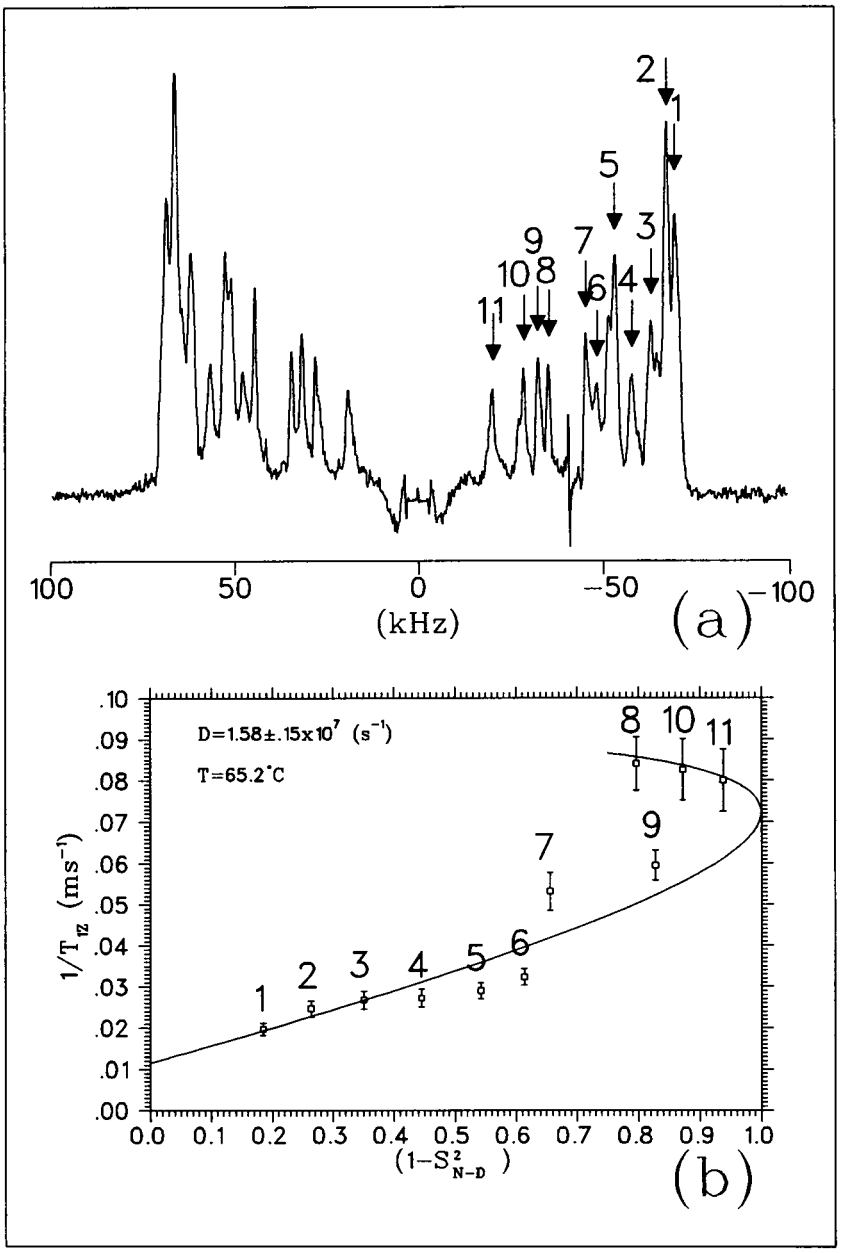

FIGURE 4 (*a*) A ^{2}H exchange-labeled gramicidin D spectrum obtained from an inversion-recovery experiment (actually the sum of spectra from the four smallest τ values) at 65°C. The numbers designate 11 distinct peaks, for which the relaxation rates $1/T_{1Z}$ were determined. In *b*, $1/T_{1Z}$, from the above-mentioned experiment, is plotted as a function of $(1 - S^2_{N-^2H})$ and the corresponding fit, assuming simply axial diffusion, is included (*solid line*). Note that the *y* intercept gives us a good estimate of the contribution to relaxation from either additional interactions or additional motional processes. Strictly speaking, the order parameters, S_{N-^2H}, were not obtained from the splittings in *a*; rather, for each peak, the first spectral moment (defined with respect to the center of the spectrum) was used to calculate the average value of S_{N-^2H}. The constants in this simulation are η (=0), e^2qQ/h (=205.9 kHz), and ω_0 (=55.265 × 10^6 × 2π s^{-1}).

correspond to N—^{2}H bonds in which θ_D is close to 90°, while peak 9 corresponds to $\theta_D \approx 40°$. Although such bond angles are inconsistent with current structural models (Prosser et al., 1994), model calculations of side chain conformations are less well known. Trp side chains may also undergo a significant amount of internal motion, which contradicts our original assumption of a rigid body undergoing only anisotropic diffusion in an orienting potential. In any case, the relaxation curve shown in Fig. 4 *b* is reasonably well defined by points 1–7. Rather than make any definite conclusions about Trp side chain conformations, we prefer to emphasize the general applicability of the above strategy of analysis for determining structural and dynamic properties of rigid integral membrane molecules. This approach is also relevant to the study of two spin-1/2 dipolar coupled systems since the T_1 relaxation expressions for two are similar in form to the corresponding expressions for quadrupolar relaxation (Spiess, 1978), (i.e., the relaxation measurements can be used in the case of these dipolar coupled spin-1/2 systems to clarify orientational information).

Our estimate for the diffusion rate is similar to that obtained by Pauls et al. (1985) by a simple T_{2E} analysis of a synthetic amphiphilic polypeptide in unoriented DPPC multilayers, while Macdonald and Seelig (1988) have obtained a lower bound estimate of $D \approx 10^8$ s^{-1} from quadrupolar-echo experiments on gramicidin (selectively labeled at the aromatic ring systems on the four tryptophan side chains) in DMPC.

As a final test of our simple model of axial diffusion, we will consider the T_{1Z} anisotropy of the outer doublet at 34°C using the above estimate for the diffusion rate. Fig. 5 *a* displays the dependence of the relaxation rate ($1/T_{1Z}$) on the

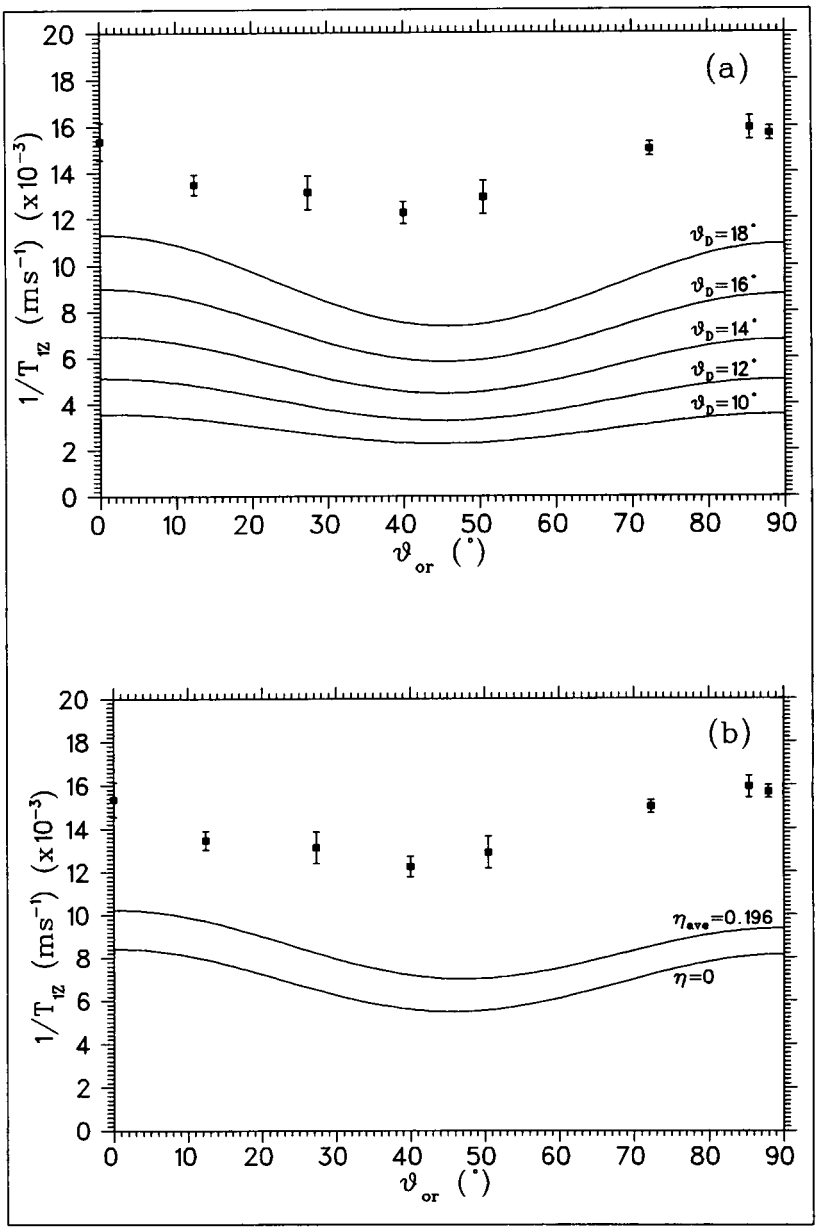

FIGURE 5 (*a*) Relaxation anisotropy ($1/T_{1Z}$ vs. θ_{or}) for the outermost doublet of ^{2}H exchange-labeled gramicidin D at 34°C. Solid lines represent the theoretical fit assuming only long axis diffusion. Here we have considered different possible Euler angles for the outermost doublet (θ_D = 10, 12, 14, or 18°). Other parameters include $D = 1.52 \times 10^7$ s^{-1}, η (=0), e^2qQ/h (=205.9 kHz), and ω_0 (=55.265 × 10^6 × 2π s^{-1}). (*b*)Average theoretical anisotropy for axial diffusion, assuming $D = 1.52 \times 10^7$ s^{-1} and ω_0 (=55.265 × 10^6 × 2π s^{-1}). In this case, the parameter set, {e^2qQ/h, η, ϕ_D, θ_D, and ψ_D}, was obtained separately from GAUSSIAN approximations (STO-3G* basis set) for each of the amides in residues 1, 3, 5, 7, 9, 11, 12, 13, and 15, for the "relaxed" Arseniev model (see Prosser (1992)) and the resulting relaxation rate anisotropies were then averaged. A comparison of the result obtained if η = 0 is also presented.

macroscopic alignment angle, θ_{or}, for the outermost doublet. From our previous lineshape analysis (Prosser et al., 1994) we have estimated that $\theta_D = 14 \pm 4°$. Assuming $\eta = 0$, the corresponding predicted relaxation anisotropy differs from the observed anisotropy in both amplitude and shape. The outer doublet arises from roughly nine separate deuteron labels (Prosser et al., 1994) all of which have slightly different quadrupole coupling constants and values of θ_D. We therefore computed the average theoretical $1/T_{1Z}$ anisotropy for axial diffusion, assuming $D = 1.52 \times 10^7$ s^{-1} and using the parameter set, {e^2qQ/h, ϕ_D, θ_D, and ψ_D}, from GAUSSIAN calculations (STO-3G* basis set) for each of the amides in residues 1, 3, 5, 7, 9, 11, 12, 13, and 15, for the "relaxed" Arseniev model (see Prosser (1992) for details). The added complication of $\eta \neq 0$ changed the theoretical anisotropy slightly. Thus, we appear to be neglecting a significant additional relaxation process. Nevertheless, the application of the axial diffusion model alone is useful since the experimental anisotropy sets an upper bound on the long axis diffusion rate (i.e., D is certainly less than 4×10^7 s^{-1}).

Long axis diffusion appears to be insufficient to explain all the features of our relaxation data. The following evidence is indicative of (an) additional slower relaxation mechanism(s):

- The apparent T_{2E} anisotropy evident in the powder spectrum of (^{2}H—C_α)Leu$_{12}$ gramicidin A in unoriented DMPC multilayers, near the phase transition (Prosser et al., 1991) was consistent with a wobbling diffusion of the peptide about the local bilayer normal, or lateral diffusion over curved surfaces.
- In all of our oriented spectra we observed a dramatic T_{2E} anisotropy (Fig. 6). We have considered three candidates for this apparent anisotropy: (i) heteronuclear ^{14}N—^{2}H

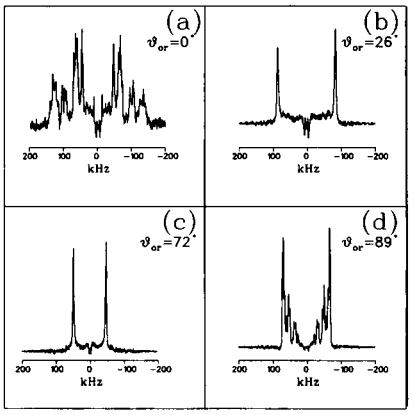

FIGURE 6 T_{1Z} spectra of ^{2}H exchange-labeled GD for plate orientations (θ_{or}) of 0 (*a*), 26 (*b*), 72 (*c*), and 89° (*d*). To improve signal to noise, each spectrum is actually the sum of spectra for the four smallest tau values in a T_{1Z} relaxation experiment (1, 2, 5, and 10 ms). The following parameters were used to obtain the above spectra: repetition time = 0.35 s, τ_1 = 35 μs, 120,000 scans, π pulse length = 7.1 μs. Note that the outer doublets in *a* are reduced by roughly a factor of three due to "radio frequency fall off" as discussed in the text.

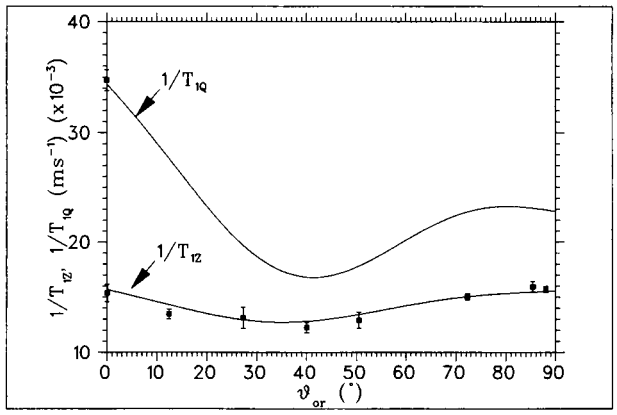

FIGURE 7 Relaxation rate anisotropy ($1/T_{1Z}$ vs. θ_{or} and $1/T_{1Q}$ vs. θ_{or}) for the outermost doublet of ^{2}H exchange-labeled gramicidin D at 34°C. The solid line represents a theoretical anisotropy profile for anisotropic diffusion in a Maier-Saupe orienting potential. The correlation times for anisotropic diffusion ($\tau_{R\|}$ and $\tau_{R\perp}$) are assumed to be 6.80 × 10^{-9} and 6 × 10^{-6} s, respectively. The ordering parameter, A_{00}, is assumed to be 4.2 and the site-specific parameters (e^2qQ/h, η, ϕ_D, θ_D, and ψ_D) are obtained from ab initio EFG calculations of gramicidin A model structures (see Prosser et al. (1994) for details) for the amide deuterons of residues 1, 3, 5, 7, 9, 11, 12, 13, and 15. The doublets corresponding to these residues are expected to comprise the broad outer doublet (Prosser et al., 1994) whose anisotropy is considered here. Note that the estimate for e^2qQ/h was obtained by multiplying the estimate from GAUSSIAN by 0.92 (Prosser et al., 1994). The other constant in this simulation is ω_0 (=55.265 × 10^6 × 2π s^{-1}).

dipolar interactions, (ii) heteronuclear ^{1}H—^{2}H dipolar interactions, and (iii) quadrupolar relaxation through a motional mechanism which is strongly T_{2E}-effective. Using a secular approximation to describe the spin Hamiltonian for the ^{2}H nucleus dipolar coupled to a single ^{14}N nucleus, Heaton et al. (1989) have calculated the quadrupolar echo amplitude as

$$E(\tau, D) = \frac{E_0}{3}[2 + \cos(4D_{dip}\tau)]$$
$$D_{dip} = -\frac{(h\gamma_D\gamma_N/2\pi r^3)(3\cos^2\theta - 1)}{2} \quad (31)$$

where E_0 is the echo amplitude at τ = 0, γ_D and γ_N are the gyromagnetic ratios of the deuteron and ^{14}N nucleus, respectively, r is the ^{2}H—^{14}N bond length, and θ is the angle between the ^{2}H—^{14}N vector and the magnetic field. Assuming a ^{2}H—^{14}N bond length of 1.03 Å, we obtain an estimate for ($h\gamma_D\gamma_N/4\pi r^3$) equal to 1320 Hz. Using Eq. 31, the heteronuclear ^{2}H—^{14}N dipolar interactions should change the amplitude of the ^{2}H quadrupole echo, for τ = 35 μs, by less than 10% of the value assuming no dipolar interactions. Heaton et al. (1989) note that the spectral distortion on the quadrupole lineshape due to this interaction increases significantly for longer values of τ. Although the ^{14}N—^{2}H dipolar interaction would be important to consider in a detailed T_{2E} anisotropy study of ^{2}H exchange-labeled GD, this interaction is not strong enough to explain the orientation dependent spectra in Fig. 6. Heteronuclear dipolar interactions between deuterons and adjacent protons have also been studied (Hing et al., 1990a,b) with GA in oriented DMPC multilayers. The authors reported that T_{2E} increased by a factor of two upon proton decoupling which can not explain our observed anisotropy. Since our oriented spectra are clearly indicative of a fast motionally symmetric regime, at least for θ_{or} = 90°, we are left with the possibility that the dramatic T_{2E} anisotropy is primarily due to an additional motion whose correlation time(s) is(are) comparable to the inverse of the quadrupole coupling constant.

- We can not simultaneously fit all of our spin-lattice relaxation experiments to a model with a single motion (axial diffusion). Clearly, our spectra are indicative of a fast motionally symmetric regime, as our relaxation simulations of long axis diffusion confirmed. Yet the T_{2E} anisotropy suggests an additional slower motion. In a previous study (Prosser et al., 1994) we observed a broadening of lipid doublets upon the addition of gramicidin D to DLPC-d_{46}. We proposed that this broadening was due to order director fluctuations or a lipid exchange on and off the peptide on a time scale comparable to the inverse of the quadrupole coupling constant.

For all of the above reasons we suggest that wobbling diffusion (Fig. 2) is a very likely relaxation mechanism for integral membrane peptides in the fluid phase.[3]

In Fig. 7 we have compared the experimental T_{1Z} anisotropy of the outer doublet to the theoretical prediction, assuming anisotropic diffusion in an orienting potential (Fig. 2 and Theory section). In this model, the simulated relaxation profile, (which assumes $\tau_{R\|}$ = 6.8 × 10^{-9} s and $\tau_{R\perp}$ = 6 ×

[3] Collective order director fluctuations are also possible; however, to distinguish between the two mechanisms would require further experiments, which are currently in progress.

10^{-6} s) agrees very well with the experimental results. The height and shape of the anisotropy prove to be sensitive to both correlation times. Note that the ratio $\tau_{R\perp}/\tau_{R\parallel}$ is considerably larger than that predicted for diffusion in an isotropic medium (Shimitzu, 1962). In Fig. 7, the theoretical relaxation anisotropy profile (of the outer doublet) is also given for $1/T_{1Q}$, using the same parameters as for $1/T_{1Z}$. Our one experimental measurement of $1/T_{1Q}$, at $\theta_{or} = 0°$, is in agreement with the prediction based upon the T_{1Z} measurements.

In a detailed study of oriented, ^{2}H exchange-labeled gramicidin A in a lyotropic nematic liquid crystalline host, Davis (1988) concluded that the rotational diffusion rate was on the order of 10^7 s^{-1}. This estimate is in close agreement with our approximation of $D = 1/6\tau_{R\parallel} = 2.5 \times 10^7$ s^{-1} and may be contrasted with the work of North and Cross (1993) who have interpreted solid state ^{15}N T_1 measurements (at two frequencies) of isotopically labeled, oriented gramicidin A, in terms of internal helical librations (Venkatachalam and Urry, 1984) and whole-body rotational diffusion. These authors conclude that the correlation time for rotational diffusion of gramicidin A in DMPC ranges between 50 and 340 ns, while the correlation time for the internal dynamics is 36 ns. North and Cross point out that their estimate of the internal dynamics is literally two to three orders of magnitude slower than that predicted by most molecular dynamics simulations (see Roux and Karplus (1988, 1991a,b) and references therein). These same authors also analyzed their data using a model which assumed restricted diffusion of the N—H vector within a cone of semiangle 10°, inside an isotropically reorienting molecule. Their simulations yielded a global and a local correlation time of 3×10^{-6} s and 6×10^{-9} s, respectively. These two times are close to the two correlation times determined in our relaxation simulation for anisotropic diffusion.

Using hydrodynamic theory we can estimate the ratio of correlation times for two cylinders of radii, r_P and r_L. For a right cylindrical integral membrane protein of radius "r" and length "h" in a membrane of viscosity "η," the characteristic correlation time for axial diffusion would be given by (Knowles and Marsh, 1991)

$$\tau_c = 2\pi\eta r^2 h/kT. \quad (32)$$

Assuming nine lipid molecules are required to form the first annulus around a peptide,[4] we estimate that the ratio $r_P/r_L = 1.9$ (i.e., $9 \times 2r_L = 2\pi \times (r_L + r_P)$). The ratio of the axial diffusion correlation time of the peptide to the lipid should then be on the order of $(r_P/r_L)^2 = 3.6$ (Knowles and Marsh, 1991). Since lipid axial diffusion rates in the presence of peptide are known to be fast on an NMR time scale (Prosser et al., 1992), we would expect the axial diffusion rate of the peptide to be fast compared to e^2qQ/h. Therefore, on both experimental and theoretical grounds, we feel that the peptide whole body dynamics may be realistically modeled by anisotropic diffusion in an orienting potential (parameterized by the two correlation times, $\tau_{R\parallel} = 6.8 \times 10^{-9}$ s and $\tau_{R\perp} \approx 6 \times 10^{-6}$ s).

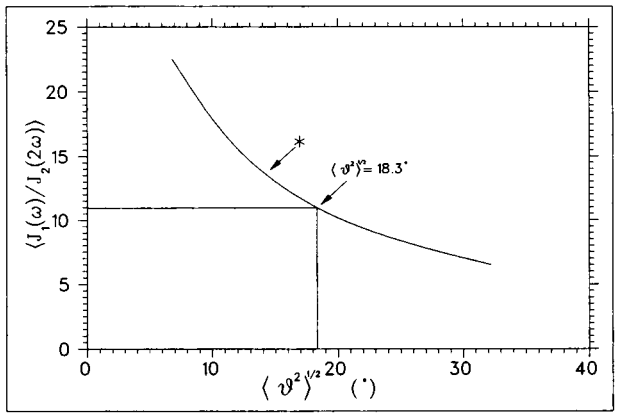

FIGURE 8 Theoretical ratio of $\langle J_1(\omega)/J_2(2\omega)\rangle$ versus the rms angle, $\langle\theta^2\rangle^{1/2}$, formed by the peptide helix axis and the local bilayer normal. The constants in this simulation are $\tau_{R\parallel} = 6.8 \times 10^{-9}$ s and $\tau_{R\perp} = 6 \times 10^{-6}$ s. Note that the ratio $\langle J_1(\omega)/J_2(2\omega)\rangle$ represents an average over nine EFG tensors, as described in Fig. 6. Our experimentally determined value of $\langle J_1(\omega)/J_2(2\omega)\rangle$ intersects the theoretical curve at $\langle\theta^2\rangle^{1/2} = 18.3°$, where $A_{00} = 3.0$. The asterisk in the figure represents the value of $\langle J_1(\omega)/J_2(2\omega)\rangle$ for which $\langle\theta^2\rangle^{1/2} = 14°$, which we obtain by first calculating $\langle T_{1Z}\rangle$ and $\langle T_{1Q}\rangle$, and then calculating the above ratio. We therefore adopt an average value for the rms angle as $\langle\theta^2\rangle^{1/2} = 16 \pm 2°$.

Few other detailed dynamics studies exist for membrane peptides or proteins. Kawato and Kinosita (1981) have discussed the application of flash-induced absorption anisotropy in the study of the dynamics of labeled membrane proteins undergoing axial diffusion and wobble, although internal wobble of the probe is in this case impossible to distinguish from wobble of the entire protein. These authors also discuss the results of experiments on cytochrome b_5, in dimyristoyl-lecithin bilayers, in which they estimate the semiangle of the cone for wobble to be 33° in both the fluid and gel phases.

Thus far, we have only been able to make a crude estimate of the molecular ordering parameter, A_{00}, from motional narrowing of the spectra. This approach is limited by our uncertainty in the exact values of the quadrupolar coupling constants and the N—^{2}H bond orientations. Although the relaxation anisotropy is very sensitive to the correlation times, it is not particularly sensitive to A_{00}. However, the ratio $J_1(\omega)/J_2(2\omega)$ (at $\theta_{or} = 0°$) is strongly dependent on A_{00} (Vold and Vold, 1991), as demonstrated in Fig. 8, where this ratio is plotted as a function of the rms angle, $\langle\theta^2\rangle^{1/2}$, formed by the peptide helix axis and the local bilayer normal, using the correlation times estimated from the above relaxation anisotropy simulation.[5] As we have described in Eq. 18, the spectral

[4] Circular dichroism experiments (Lograsso et al., 1988) reveal a significant change in the circular dichroism trace when the lipid to protein ratio is less than 8.5:1 which is presumably the point at which there is no longer enough lipid to form a single annulus around a given peptide.

[5] The scrutinizing reader may worry that if $J_1(\omega)/J_2(2\omega)$ is strongly a function of the correlation times, then the estimate of A_{00}, obtained from an experimental measure of this ratio, is only as good as the estimate of the correlation times. Fortunately, $J_1(\omega)/J_2(2\omega)$ is not particularly sensitive to the motional rates (Vold and Vold, 1991).

densities $J_1(\omega)$ and $J_2(2\omega)$ may be independently obtained from separate measurements of T_{1Z} and T_{1Q}. Moreover, the ratio, $J_1(\omega)/J_2(2\omega)$, can be obtained from these relaxation times, without the knowledge of e^2qQ/h, thus permitting an accurate estimate of A_{00}. The only complication, which arises from the fact that we employed an exchange-labeled sample, is that the outer doublet is composed of roughly nine independent labels. Thus to produce the theoretical profile in Fig. 8, we calculated $\langle J_1(\omega)/J_2(2\omega)\rangle$, averaged over nine EFG tensors. Fig. 8 shows the experimental measure of $J_1(\omega)/J_2(2\omega)$ intersecting the theoretical profile, where $A_{00} \approx 3.0$. This corresponds to a rms angle $\langle\theta^2\rangle^{1/2} = 18°$ formed by the peptide helix axis and the average bilayer normal. This angle is slightly higher than that predicted by either our motional narrowing estimate of 14° (Prosser et al., 1994) or the order parameter estimate of Separovic et al. (1993). In fact, if we separately calculate average values of T_{1Z} and T_{1Q} from the nine EFG tensors which we expect to contribute to the outer most doublet, we obtain an rms angle of $\langle\theta^2\rangle^{1/2} = 14°$ ($A_{00} = 4.2$). Taking an average of the above two estimates for $\langle\theta^2\rangle^{1/2}$, we obtain a final estimate of $\langle\theta^2\rangle^{1/2} = 16 \pm 2°$. Lastly, we note that Vold and Vold (1991) have constructed a similar simulation of J_1/J_2 for wobble in a cone of semiangle, θ_s. Under this model, our measurement suggests that $\theta_s \approx 30°$.

CONCLUSIONS

In this paper, we have analyzed detailed T_{1Z} and T_{1Q} relaxation data from ^{2}H exchange-labeled gramicidin D in oriented DLPC multilayers in order to address the dynamic properties of the integral membrane peptide. The decay of each doublet in the inversion-recovery spectra is characterized by T_{1Z}, which is inversely proportional to the sum of the spectral density functions $J_1(\omega_0) + 4J_2(2\omega_0)$, where ω_0 equals the Larmor frequency. The motional narrowing factor, obtained from the spectra, permitted us to estimate the molecular order parameter which is directly related to the strength of the restoring potential, A_{00}, in which the peptide is presumed to undergo long axis and wobbling diffusion (characterized by the correlation times, $\tau_{R\parallel}$ and $\tau_{R\perp}$). By graphing the relaxation rate, $1/T_{1Z}$, as a function of $(1 - S^2_{N-^2H})$, for $\theta_{or} = 90°$, we were able to estimate the correlation time, $\tau_{R\parallel}$, for long axis diffusion, under the assumption that long axis diffusion was the dominant relaxation contribution. Although in general, the quadrupolar splitting, which is a function of $(3\cos^2\theta_D - 1)$, has two possible solutions to θ_D in the range $0 \le \theta_D \le 90°$, the $1/T_{1Z}$ vs. $(1 - S^2_{N-^2H})$ curve can be used to determine a single value of θ_D in this range. Thus, the $1/T_{1Z}$ vs. $(1 - S^2_{N-^2H})$ curve is useful for defining the long axis diffusion rate and removing potential structural ambiguities in the splittings. The same parameters, obtained from the $1/T_{1Z}$ vs. $(1 - S^2_{N-^2H})$ curves, could not fully reproduce the observed $1/T_{1Z}$ anisotropy. In addition, the reduction in the splitting from what we would expect in the absence of motions other than axial diffusion, and the strong $(1 - S^2_{N-^2H})$ dependence of $1/T_{2E}$, all point to an additional motion whose correlation time is slow on the T_{1Z} time scale. In this paper we propose this additional motion to be whole body wobbling diffusion, and we have attempted to explain all of our relaxation data in terms of anisotropic diffusion in a Maier-Saupe restoring potential. This model has been proposed before to explain relaxation data of lipids and cholesterol in membranes (Mayer et al., 1988, 1990; Weisz et al., 1992).

We would like to point out that by using a rigid molecule whose various labels sample many orientations at once, one can in principle simultaneously determine unambiguous orientational information about all of the labels and determine the correlation time associated with the dynamics of the rigid body. Even if wobble (diffusion of the molecule about an axis perpendicular to the local bilayer normal) is a significant relaxation process, our simulations reveal that its contributions to the spin-lattice relaxation rates are minimized at macroscopic sample orientations of $\theta_{or} = 90°$.

Analysis of the relaxation anisotropy at 34°C permitted us to estimate the correlation times for long axis and wobbling diffusion of the entire peptide, as 6.8×10^{-9} and 6×10^{-6} s. This fit was corroborated by a Jeener-Broekaert experiment at $\theta_{or} = 0°$. Finally, the measurement of T_{1Z} and T_{1Q} at $\theta_{or} = 0°$ and 34°C, permitted us to estimate (independent of the knowledge of the quadrupole coupling constants) the rms angle, $\langle\theta^2\rangle^{1/2}$ (formed by the peptide helix axis and the local bilayer normal), as $16 \pm 2°$.

Ultimately, we would like to obtain an accurate theoretical description of the structural and dynamical features of gramicidin. Detailed stochastic boundary molecular dynamics simulations of phospholipid bilayers are now emerging (Pastor, 1990; Pastor et al., 1991; De Loof et al., 1991) despite the "inherent difficulties caused by (i) the dynamic nature of the liquid-crystalline state, requiring the calculation of multinanosecond trajectories; (ii) the large dimensions and heterogeneous composition of membranes; (iii) and the complex, often curved or highly charged interface requiring a sophisticated treatment of boundary conditions and electrostatics" (De Loof et al., 1991). One such multinanosecond simulation of a phospholipid in a fluid bilayer combined Langevin dynamics (with a Marcelja-based mean field at the boundary) on a hexagonally packed seven-lipid array, with classical MD (and no mean field) on the central DPPC molecule (De Loof et al., 1991). This methodology is currently being extended to gramicidin (in the membrane) (B. Roux, personal communication). NMR measurements of average bond orientations, order parameters, correlation times, and motional activation energies reflect the essential physical interactions between the lipid milieu and the peptide. It is our hope that the union of Langevin molecular dynamics simulations with comprehensive relaxation studies will advance our understanding of the essential interactions which dictate membrane protein structure, and facilitate simulations of larger membrane proteins.

Many thanks to Prof. Mike Morrow for helpful comments and to Denis Langlais for help preparing this manuscript.
This work was supported by grants from the Natural Sciences and Engineering Research Council of Canada.

REFERENCES

Brooks, C. L., M. Karplus, and B. M. Pettitt. 1988. *Proteins: A Theoretical Perspective of Dynamics, Structure, and Thermodynamics*, in *Advances in Chemical Physics*, vol 71 Prigogine, I., and Rice, S. A., Eds., John Wiley and Sons, New York.

Cotter, M. A. 1977. Hard spherocylinders in an anisotropic mean field: A simple model for a nematic liquid crystal. *J. Chem. Phys.* 66:1098–1106.

Davis, J. H. 1983. The description of membrane lipid conformation, order and dynamics by ^{2}H-NMR. *Biochim. Biophys. Acta.* 737:117–171.

Davis, J. H. 1988. ^{2}H NMR of exchange-labeled gramicidin in an oriented lyotropic nematic phase. *Biochemistry.* 27:428–436.

Davis, J. H. 1991. Deuterium magnetic resonance spectroscopy in partially ordered systems. In *Isotopes in the Physical and Biomedical Sciences*, Vol. 2, Buncel, E., and Jones, J. R., Eds., Elsevier, Amsterdam.

Davis, J. H. 1993. The molecular dynamics, orientational order and thermodynamic phase equilibria of cholesterol/phosphatidylcholine mixtures: ^{2}H NMR. *In* Cholesterol in Membrane Models. L. Finegold, editor. CRC Press, Boca Raton, Florida. 67–136.

Davis, J. H., K. R. Jeffrey, M. Bloom, M. I. Valic, and T. P. Higgs. 1976. Quadrupolar echo deuteron magnetic resonance spectroscopy in ordered hydrocarbon chains. *Chem. Phys. Lett.* 42:390–394.

De Loof, H., S. C. Harvey, J. P. Segrest, and R. W. Pastor. 1991. Mean field stochastic boundary molecular dynamics simulation of a phospholipid in a membrane. *Biochemistry.* 30:2099–2113.

Heaton, N. J., R. R. Vold, and R. L. Vold. 1989. Heteronuclear dipolar dephasing of deuterium quadrupole echoes. *J. Chem. Phys.* 91:56–62.

Hing, A. W., S. P. Adams, D. F. Silbert, and R. E. Norberg. 1990. Deuterium NMR of Val^1···(2-^{2}H)Ala^3···gramicidin A in oriented DMPC bilayers. *Biochemistry.* 29:4144–4156.

Hing, A. W., S. P. Adams, D. F. Silbert, and R. E. Norberg. 1990. Deuterium NMR of ^{2}*H*CO-Val^1···gramicidin A and ^{2}*H*CO-Val^1-D-Leu^2···gramicidin A in oriented DMPC bilayers. *Biochemistry.* 29:4156–4166.

Jackson, J. D. 1975. *Classical Electrodynamics*, John Wiley and Sons, New York.

Jeffrey, K. R. 1981. Nuclear magnetic relaxation in a spin one system. *Bull. Mag. Res.* 3:69–82.

Kawato, S., and K. Kinosita. 1981. Time-Dependant Absorption of Anisotropy and Rotational Diffusion of Proteins in Membranes. *Biophys. J.* 36:277–296.

Knowles, P. F., and D. Marsh. 1991. Magnetic resonance of membranes. *Biochem. J.* 274:625–641.

LoGrasso, P., F. Moll, and T. A. Cross. 1988. Solvent History of Gramicidin A Conformations in Hydrated Lipid Bilayers. *Biophys. J.* 54:259–267.

Macdonald, P. M., and J. Seelig. 1988. Dynamic properties of gramicidin A in phospholipid membranes. *Biochemistry.* 27:2357–2364.

Mayer, C., G. Gröbner, K. Müller, K. Weisz, and G. Kothe. 1990. Orientation-dependent spin-lattice relaxation times in bilayer membranes: characterization of the overall lipid motion. *Chem. Phys. Lett.* 165:155–161.

Mayer, C., K. Müller, K. Weisz, and G. Kothe. 1988. Deuteron NMR relaxation studies of phospholipid membranes. *Liquid Cryst.* 3:797–806.

McCammon, J. A., and S. C. Harvey. 1987. *Dynamics of Proteins and Nucleic Acids*, Cambridge Univ. Press, Cambridge.

Millar, J. M., A. M. Thayer, H. Zimmerman, and A. Pines. 1986. High-resolution studies of deuterium by time-domain zero-field NQR. *J. Magn. Res.* 69:243–257.

North, C. L., and T. A. Cross. 1993. Analysis of the polypeptide backbone T_1 relaxation data using an experimentally derived model. *J. Magn. Res.* In Press.

Pastor, R. W. 1990. In *Molecular Description of Biological Membrane Components by Computer Aided Conformational Analysis*, Brasseur, R., Ed., Vol. 1, 171–201, CRC Press, Boca Raton, Florida.

Pastor, R., R. Venable, and M. Karplus. 1991. Model for the structure of the lipid bilayer. *Proc. Natl. Acad. Sci. USA.* 88:892–896.

Pauls, K. P., A. L. MacKay, O. Söderman, M. Bloom, A. K. Tanjea, and R. S. Hodges. 1985. Dynamic properties of the backbone of an integral membrane polypeptide measured by ^{2}H NMR. *Eur. Biophys. J.* 12:1–11.

Prosser, R. S. 1992. The structure and dynamics of an amphiphilic peptide: A deuterium NMR relaxation study of gramicidin A. PhD Thesis. University of Guelph.

Prosser, R. S., S. I. Daleman, and J. H. Davis. 1994. The structure of an integral membrane peptide: A deuterium NMR study. *Biophys. J.* 66:1415–1428.

Prosser, R. S., J. H. Davis, F. W. Dahlquist, and M. A. Lindorfer. 1991. ^{2}H NMR of the gramicidin A backbone in a phospholipid bilayer. *Biochemistry.* 30:4687–4696.

Prosser, R. S., J. H. Davis, C. Mayer, K. Weisz, and G. Kothe. 1992. Deuterium NMR relaxation studies of peptide-lipid interactions. *Biochemistry.* 31:9355–9363.

Rommel, E., F. Noack, P. Meier, and G. Kothe. 1988. Proton spin relaxation dispersion studies of phospholipid membranes. *J. Phys. Chem.* 92: 2981–2987.

Roux, B., and M. Karplus. 1988. The normal modes of the gramicidin-A dimer channel. *Biophys. J.* 53:297–309.

Roux, B., and M. Karplus. 1991a. Ion transport in a gramicidin-like channel: Dynamics and mobility. *J. Phys. Chem.* 95:4856–4868.

Roux, B., and M. Karplus. 1991b. Ion transport in a model gramicidin channel. *Biophys. J.* 59:961–981.

Separovic, F., R. Pax, and B. Cornell. 1993. NMR order parameter analysis of a peptide plane in a lyotropic liquid crystal. *Mol. Phys.* 78:357–369.

Shimitzu, H. 1962. Effect of molecular shape on nuclear magnetic relaxation. *J. Chem. Phys.* 37:765–778.

Spiess, H. W. 1978. *Rotation of Molecules and Nuclear Spin Relaxation* in *NMR Basic Principles and Progress*, Diehl, P., Fluck, E., and Kosfeld, K., Eds., Springer-Verlag, New York, 15:55–214.

Venkatachalam, C. M., and D. W. Urry. 1984. Theoretical analysis of the gramicidin A transmembrane channel. II. Energetics of helical librational states of the channel. *J. Comput. Chem.* 5:64–71.

Vold, R. R., and R. L. Vold. 1988. Nuclear spin relaxation and molecular dynamics in ordered systems: Models for molecular reorientation in thermotropic liquid crystals. *J. Chem. Phys.* 88:1443–1457.

Vold, R. R., and R. L. Vold. 1991. Deuterium relaxation in molecular solids. In *Advances in Magnetic and Optical Resonance*, Vol. 16, pp. 85–171, Warren, W., Ed., Academic Press, New York.

Weisz, K., G. Gröbner, C. Mayer, J. Stohrer, and G. Kothe. 1992. Deuteron NMR study of the dynamic organization of phospholipid/cholesterol bilayer membranes: molecular properties and viscoelastic behavior. *Biochemistry.* 31:1100–1112.

Wittebort, R. J., and A. Szabo. 1978. Theory of NMR relaxation in macromolecules: Restricted diffusion and jump models for multiple internal rotations in amino acid side chains. *J. Chem. Phys.* 69:1722–1736.